MIT Open Access Articles

A designed amphiphilic peptide containing the silk fibroin motif as a potential carrier of hydrophobic drugs

A designed amphiphilic peptide containing the silk fibroin motif as a potential carrier of hydrophobic drugs

Qinghan Zhou [a], Juan Lin [a], Jing Wang [a], Feng Li [a], Fushan Tang [a], Xiaojun Zhao [a,b,c,*]

[a] *Institute for Nanobiomedical Technology and Membrane Biology, West China Hospital, Sichuan University, Chengdu 610041, China*
[b] *State Key Lab of Biotherapy of Human Diseases, Cancer Center, West China Medical School, West China Hospital, Sichuan University, Chengdu 610041, China*
[c] *Center for Biomedical Engineering NE47-378, Massachusetts Institute of Technology, MA 02139-4307, USA*

Abstract

The amphiphilic peptide is becoming attractive as a potential drug carrier to improve the dissolvability of hydrophobic drugs in an aqueous system; thus, facilitating drug uptake by target cells. Here, we report a novel designed amphiphilic peptide, Ac-RADAGAGA-RADAGAGA-NH$_2$, which was able to stabilize pyrene, a hydrophobic model drug we chose to study in aqueous solution. This designed peptide formed a colloidal suspension by encapsulating pyrene inside the peptide–pyrene complex. Egg phosphatidylcholine (EPC) vesicles were used to mimic cell bilayer membranes. We found that pyrene was released from the peptide coating into the EPC vesicles by mixing the colloidal suspension with EPC vesicles, which was followed by steady fluorescence spectra as a function of time. A calibration curve for the amount of pyrene released into the EPC vesicles at a given time was used to determine the final concentration of pyrene released into the lipid vesicles from the peptide–pyrene complex. The release rate of the peptide–pyrene complex was calculated to quantify the transfer of pyrene into EPC vesicles.

© 2009 National Natural Science Foundation of China and Chinese Academy of Sciences. Published by Elsevier Limited and Science in China Press. All rights reserved.

Keywords: Pyrene; Hydrophobicity; Drug carrier; Fluorescence; Amphiphilic peptide

1. Introduction

The self-assembly phenomenon of peptides bearing different sequences in an aqueous solution was discovered over 10 years ago [1] and prompted numerous studies of various nanostructures of such peptides [2–6]. Self-assembly peptides have been used in many applications such as 3D cell cultures [7], tissue or organ injury repair systems [8], biological surface engineering [9], and membrane protein stabilization [10]. In recent years, the study of self-assembly peptides as hydrophobic drug carriers has attracted great interest from scientists, and several types of peptides have been reported to be useful in the potential application of drug delivery systems [11–13]. To broaden this field, and to improve the compatibility between peptides and hydrophobic drugs, other types of peptides should be designed and investigated.

As native proteins, silk fibroins have been proven to be useful in drug delivery because of their good biocompatibility, hydrophobicity, and porous network structure [14–16]. Poly-GA (where G is Glycine, and A is Alanine) is a prevalent conservative motif in silk protein, particularly in silk produced by the silk moth *Bombyx mori*. This peptide occupies 40–50% of the total volume of the silk fiber [17]. In silk fibroin, the GA motif forms a packed structure via hydrophobic interactions [18], which facilitates the formation of networks in the silk

---

* Corresponding author. Tel.: +86 28 85164069; fax: +86 28 85164072.
  E-mail address: xjzhao.scu@gmail.com (X. Zhao).

fiber [19]. Because of the high content of the GA motif in silk protein, it is likely that the GA motif can play an important role in the use of silk proteins in drug delivery systems. However, the hydrophobicity of the GA motif means low solubility of peptides such as $(GA)_n$ and G_nA_m in water. Therefore, to design an amphiphilic peptide containing the GA motif, it is important to achieve this goal.

RADA16-I, Ac-RADARADARADARADA-NH$_2$, is a typical ionic self-complementary peptide with two distinct surfaces—one hydrophilic, the other hydrophobic. It comprises 16 amino acids with alternating positively and negatively charged amino acids, which are separated by a hydrophobic amino acid [20]. The peptide, which has a β-sheet secondary structure, can self-assemble into nanofiber scaffolds after being dissolved in an aqueous solution. Furthermore, the peptide has been studied in many applications, including 3D cell culture [21] and tissue recovery [22]. Because of its good solubility in water and fibrous structure, in this study, an amphiphilic peptide containing the GA motif was designed based on the amino acid sequence of RADA16-I. And its potential use as a drug carrier was investigated.

We studied whether the novel peptide can stabilize pyrene crystals (a hydrophobic drug model) in water, because pyrene shows very poor dissolution in water, which leads to difficulties in achieving delivery of drugs to the target cell or location via body fluid circulation. We further studied whether the peptide could deliver pyrene into the bilayer membranes of egg phosphatidylcholine (EPC) vesicles as carriers. Because of the well-characterized fluorescence of pyrene [23], steady-state fluorescence spectroscopy was used to obtain information about the interaction of the peptide with pyrene. We used atomic force microscopy (AFM) to investigate the self-assembling nanostructure of the peptide, and dynamic light scattering (DLS) to determine the size distributions of EPC vesicles.

2. Materials and methods

2.1. Materials

The peptide, Ac-RADAGAGARADAGAGA-NH$_2$ (1399.41 g/mol), which was commercially synthesized and purified (>95%) (Bootech BioScience & Technology Co., Ltd, Shanghai, China) was acetylated at N termini and amidated at C termini. Egg phosphatidylcholine (EPC) was purchased from Sinopharm Chemical Reagents Co., Ltd, Shenyang, China. Pyrene (99%) was obtained from Sigma–Aldrich and was recrystallized from ethanol before the experiment. The rest of the chemicals used in the experiment were acquired from Chengdu Kelong Chemical Reagents Co., Chengdu, China. All the aqueous solutions were prepared using deionized water (ElixWater Purification System, Millipore, MA, USA).

2.2. EPC vesicle preparation

EPC (0.8 g) was dissolved in chloroform. The organic solvent was evaporated by a rotary evaporator at 25 °C to produce an EPC thin film inside the round-bottom flask. Then, the EPC film was exposed to high vacuum for at least 2 h to remove any trace of chloroform and was resuspended in 300 ml of buffer solution (pH 7.4, containing 25 mM Tris–HCl acid and 0.2 mM EDTA). After being bubbled with nitrogen, the mixture was sonicated for half an hour at 0 °C by a ultrasonic crasher set at about 200 W output. This was followed by centrifugation at 12,000 g for 1.5 h. The supernatant was filtered by 0.44 and 0.22 μm membrane filters in turn. Liposome size was measured by the Malvern Zetasizer Nano ZS analyzer.

2.3. Determination of the lipid concentration

One milliliter of the vesicle solution was pipetted into each of three pre-weighed 20 ml vials. Tris–HCl acid and EDTA buffer solution with the same volume were pipetted into another three pre-weighed 20 ml vials. The three sets of vesicle and buffer solutions were dried under a stream of nitrogen to obtain a film at the bottom of the vial. The vials were then placed in a vacuum oven overnight at 60 °C to remove any trace of water. The mass of vesicles was obtained by mass subtraction of two sets, and the average concentration of the vesicles in the buffer solution was calculated. The deviation from the average concentration was consistently less than 2.0%.

2.4. Preparation of colloidal suspensions of pyrene crystals

An appropriate amount of pyrene was dissolved in tetrahydrofuran, placed into a 10-ml vial, and dried under a continuous stream of nitrogen. A freshly prepared peptide solution was added to this vial and diluted with deionized water to obtain the expected concentration of the solution. The peptide–pyrene solution was prepared to a final concentration of 0.53 mg/ml (3.79×10^{-4} M) for the peptide and 0.9 mg/ml (4.45×10^{-3} M) for pyrene. The sample solution was stirred for 5 days until an equilibrium was reached. The solutions were deemed to have reached equilibrium when their fluorescence spectra did not change over 24 h.

2.5. Atom force microscope (AFM) observation

The peptide solution at a concentration of 1 mg/ml was used. Five microliters of the sample was deposited onto a freshly cleaved mica substrate. Each aliquot was left on the mica for 1 min, then washed with deionized water, and dried in air for about 20 min. The images were obtained by scanning the mica surface in air by AFM (SPA400, SII Nanotechnology, Inc.) operating in tapping mode. Soft silicon cantilevers were chosen with a cantilever length of 200 μm, a spring constant of 12 N/m, and a tip

radius of curvature of 10 nm. The scans were taken at a 512×512-pixels resolution and produced topographic images of the samples in which the brightness of the features increases as a function of height. Typical scanning parameters were as follows: vibrating frequency $\sim$124 kHz, integral and proportional gains 0.1–0.4 and 0.01–0.03, respectively, amplitude reference −0.1 to −0.25, and scanning speed 0.8–1.2 Hz.

2.6. CD measurement

The circular dichroism (CD) spectra were obtained using the sample solution at a concentration of 0.125 mg/ml. The CD spectrum between 190 and 260 nm was collected with the wavelength scan mode on a Model 400 Circular Dichroism Spectrophotometer (Aviv Biomedical, Inc.) at 20 °C. A quartz cell of 0.1 cm optical path length was chosen to hold the sample solution and placed in a chamber flushed with N_2. Every sample was scanned three times, and the spectra signal was averaged and smoothed.

2.7. Steady-state fluorescence measurements

Fluorescence spectra were recorded on a Hitachi F-7000 FL fluorophotometer at room temperature. Solution samples were operated in a quartz fluorescence cuvette of 1×1 cm cross-section, while solid samples were carried out by using a solid accessory. Excitation and emission slits were set to 5 and 2.5 nm, respectively. By setting the excitation wavelength at 336 nm, the emission fluorescence spectra were scanned from 350 to 650 nm, with a scan speed of 1200 nm/min. Excitation spectra were recorded at the selected emission wavelengths (374 and 470 nm).

2.8. Calibration curve

Solutions of pyrene in EPC vesicles with pyrene concentrations ranging from 10^{-6} to 1.4×10^{-4} M and an EPC concentration of 6.99×10^{-4} M were prepared by placing an appropriate amount of pyrene dissolved in THF into a 10 ml vial, and the solution was evaporated under a stream of nitrogen to produce a film of pyrene at the bottom of the vial. The pyrene was then dissolved in 3 ml of vesicle solution referred to as EPC–pyrene solutions. The I_m (fluorescence intensity of the pyrene monomer) for the EPC–pyrene samples was obtained by averaging the emission intensities of the pyrene monomer for the EPC–pyrene solutions monitored at 374 nm for 120 s. In order to avoid the influence of xenon lamp fluctuations, the intensity of the pyrene monomer standard (I_s) is needed. A degassed and sealed solution of pyrene dissolved in ethanol ($[PY] = 3.85 \times 10^{-5}$ M) was monitored at 374 nm for 120 s, and the measured intensity was averaged to yield I_s after each spectrum of the EPC–PY solutions. The corrected value of the monomer intensity (I_m/I_s) for the EPC–PY solutions was obtained by dividing I_m by I_s.

2.9. Dynamic light scattering measurement (DLS)

The sample solution of 600 μl was used to perform the measurement. The size distribution was determined by using a laser diffraction particle sizer (Nano-ZS90, Malvern). Each sample was ultrasonicated for 30 min using an ultrasonic cleaner, and a low volume disposable sizing cuvette was chosen to hold the sample solution. The intensity for each sample was collected in three replicates and yielded the size-fraction distribution plots. The temperature was kept at 25 °C during measurement.

3. Results and discussion

3.1. Peptide nanofibers and preparation of colloidal suspensions of pyrene crystals

The peptide, Ac-RADAGAGARADAGAGA-NH$_2$, was commercially synthesized as a lyophilized powder. Before each experiment, the peptide was mixed with deionized water and stored at 4 °C overnight. The fibrous nanostructure was observed using AFM and TEM, as shown in Fig. 1. The peptide solution was clear with a pH of 3.5. Based on the AMF images, the average length of nanofibers was 4 μm and the diameter was 90 nm. CD was used to measure the secondary structure of the peptide. The CD spectra of the amphiphilic peptide revealed a strong negative peak at 194 nm and a weaker negative peak at 223 nm, which represented neither an α-helix nor β-sheet structure (data not shown). This type of CD spectra has been indicated to represent random-coil secondary structures in some reports [24].

Pyrene was chosen as the hydrophobic model drug in this experiment because of its low solubility and wide application as a molecular probe [25]. No static pyrene excimer formed in the liposomes, as reported by Winnik [26], which facilitated detection of the delivery of pyrene into the phospholipid bilayer. An appropriate amount of peptide solution was mixed with pyrene, while the same volume of deionized water was added to the control sample. After stirring for 2 h, the peptide–pyrene solution became turbid and milky-white in color, which suggested a colloidal suspension was obtained. However, because of the low solubility of pyrene (about 6.0×10^{-7} M in a saturated aqueous solution [23]), the control sample without peptide was still clear, with pyrene crystals floating on the top or precipitating at the bottom (Fig. 2). The sample solution was deemed to have reached equilibrium after stirring for 5 days, as indicated by a lack of change in fluorescence spectra over 24 h. The pH of the peptide–pyrene solution was about 3.48, which was similar to that of the peptide in water. The formation of a colloidal suspension suggested that the peptide had stabilized the pyrene crystals in the aqueous solution (4.45×10^{-3} M). Aggregation of a drug in an aqueous system would prevent delivery of the drugs to the target cells or location via body fluid circulation; therefore, the stabilization of the pyrene crystal means the likelihood for
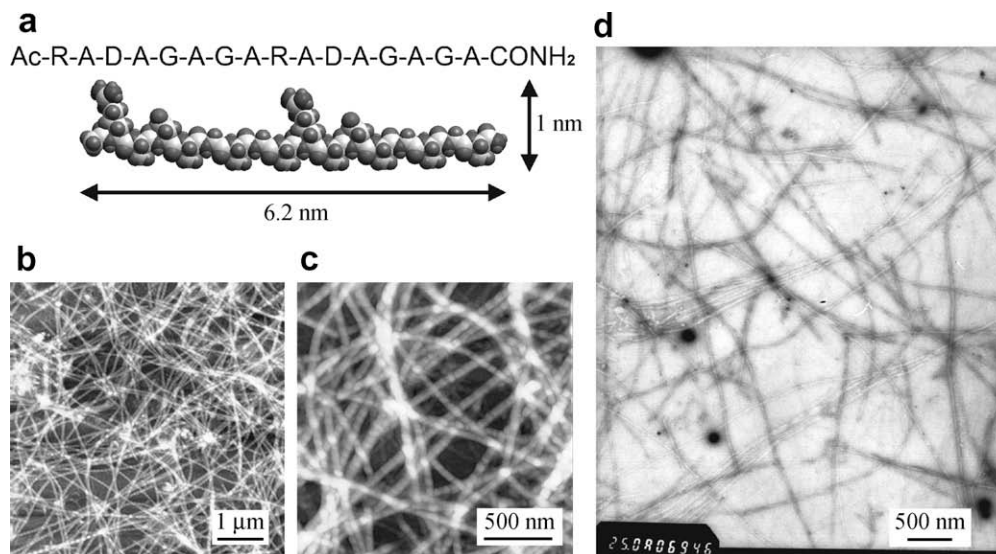
Fig. 1. (a) Amino acid sequence of the self-assembly peptide and space-filling molecular model of a peptide approximately 6.2 nm long, 1 nm wide, and 0.5 nm thick. (b) and (c) show AFM images of the peptide nanofiber in water at different scales, 6×6 μm (b), 2×2 μm (c). (d) TEM photo of the peptide nanofiber in water at a concentration of 1 mg/ml.

Fig. 2. Pyrene ([Py] = 4.45×10^{-3} M) in deionized water (left), and the peptide–pyrene solution ([Py] = 4.45×10^{-3} M, [Peptide] = 3.79×10^{-4} M) (right) after stirring for about 2 h.

achieving delivery of drugs. After the formation of the peptide–pyrene colloidal suspension, fiber-like peptides were still found in the sample solution, which had a lower density than that of the peptide in water at the same concentration according to findings of the AFM observation. It seems likely that the pyrene interacted with the hydrophobic region of the peptide and formed a peptide–pyrene complex, which decreased the formation of peptide nanofibers. However, this finding needs to be further evaluated.

3.2. Transfer of pyrene into the EPC vesicles

In order to target living cells, the hydrophobic drug must cross the cell membrane. As lipids are the essential components of cell membranes, we used EPC vesicles as a model membrane to investigate whether the pyrene molecules could be transferred into the lipid vesicles by peptide carriers. The size distribution of the prepared EPC vesicles was determined by dynamic light scattering. The dynamic diameter of the vesicles ranged from 50 to 100 nm with an average diameter of 75 nm, which were defined as large unilamellar vesicles (LUVs) as reported in Ref. [12]. The fluorescence spectra of the pyrene crystals and peptide–pyrene solution at equilibrium were obtained using a fluorophotometer. To investigate whether the transfer occurred, a sample of the peptide–pyrene solution mixed with EPC vesicles and a sample of pure pyrene in EPC vesicles were used. The steady-state fluorescence spectra are shown in Fig. 3.

Mizusaki et al. [27] reported that pyrene monomers exhibited five emission bands between 375 and 400 nm, which were attributed to the emission of spatially isolated pyrene groups, and this character could be used to identify the pyrene monomer from the pyrene crystals. No emission corresponding to pyrene monomers was found in the steady-state fluorescence spectra of pyrene crystals and the peptide–pyrene solution, but a broad featureless band was observed at around 470 nm, which is attributed to pyrene excimer emission. Emission corresponding to the pyrene monomer was observed in the spectra for pyrene in the EPC vesicles and the peptide–pyrene solution mixed with the vesicles, which were rather similar. According to previous reports, the emission intensity ratio of the first (374 nm) to the third (385 nm) peak (I_1/I_3) is usually considered as a polarity measurement of the pyrene microenvironment [28]. This ratio equals 1.96 in polar solvents such as water and decreases with increasing solvent apolarity. In this experiment, the I_1/I_3 ratio of pyrene in EPC vesicles and peptide–pyrene mixed with EPC were both 1.1, which
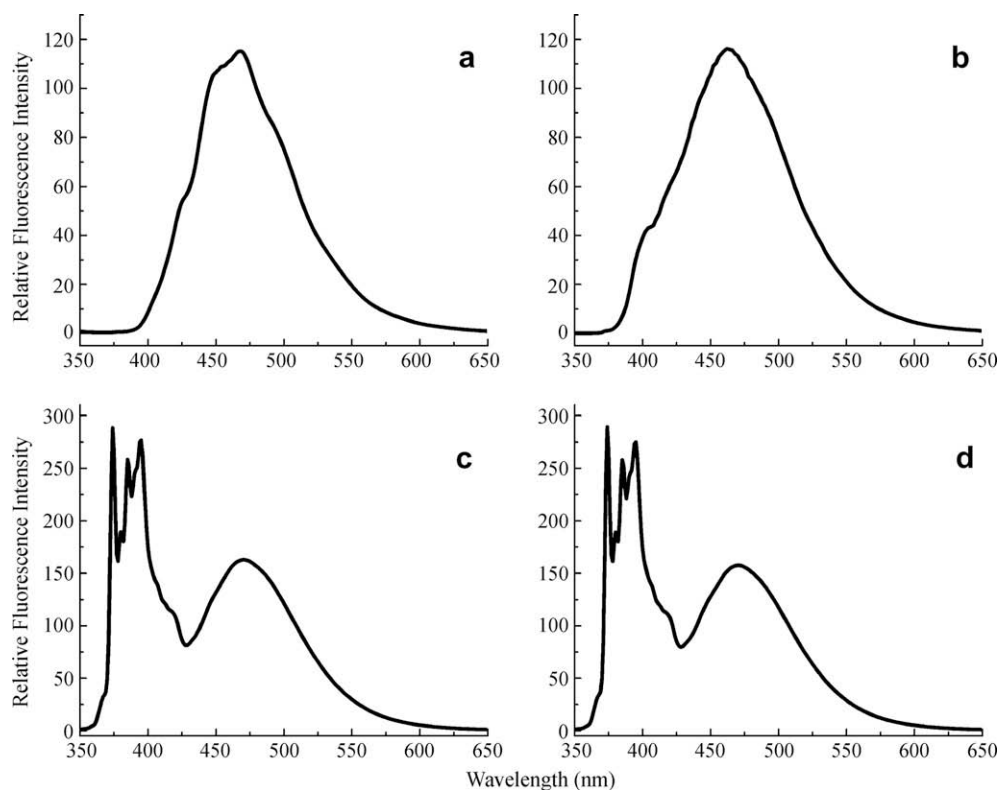
Fig. 3. Fluorescence emission spectra of solid pyrene crystals (a), peptide–pyrene solution ([Py] = 4.45×10^{-3} M, [Peptide] = 3.79×10^{-4} M) (b), pyrene in EPC vesicles ([Py] = 5.00×10^{-5} M) (c), and peptide–pyrene solution mixed with EPC vesicles ([Py] = 4.45×10^{-5} M, [Peptide] = 3.79×10^{-6} M) (d). The excitation wavelength was 336 nm. The excitation slit width and emission slit width for the solid pyrene crystals were 5 and 2.5 nm, respectively.

is in good agreement with the published I_1/I_3 value in lipid vesicles. This provided further evidence that pyrene had transferred into the cell membrane model from the peptide coating. Moreover, the ratio of the emission intensity between the excimer at about 470 nm and the monomer emission maxima at about 374 nm (I_e/I_m) can be used to estimate the local viscosity in the host [29]. In this regard, Ringsdorf et al. [30] used the ratio of pyrene excimer emission intensity and locally excited pyrene emission intensity (I_e/I_m) as a structure indicator for characterizing high local pyrene concentration inside the liposome. In this experiment, both spectra exhibited a very similar ratio I_e/I_m of 0.55 for peptide–pyrene in EPC vesicles and 0.56 for pyrene crystals in EPC vesicles, which indicated a similar excimer emission intensity of the two systems in phospholipid bilayers.

Because excimers were observed in the steady-state fluorescence spectra of both the pyrene crystals and the pyrene in EPC vesicles, additional studies are needed to determine whether the transfer of pyrene into EPC vesicles had occurred. It has been reported that the pyrene excimer has two forms: one is a dynamic excimer that is formed via diffusional encounters between pyrene molecules, and the other is a ground-state pyrenean static excimer that is formed from the direct excitation of ground-state pyrene dimers [31]. Thus, excitation spectra were investigated. According to a previous study [32], the static excimer has

a red-shift excitation spectrum, and the dynamic excimer has the same excitation spectrum as that of monomer emission (at the selected emission wavelength $\lambda_{em} = 374$ nm and $\lambda_{em} = 470$ nm). The fluorescence spectra obtained are shown in Fig. 4.

As shown in Fig. 4(a) and (b), as compared with the excitation spectrum monitored at monomer emission, the excitation spectra of solid pyrene crystals and peptide–pyrene at the excimer emission region were red-shifted by about 35 nm from 333 to 368 nm. However, no shifts were observed in the spectra of pyrene and peptide–pyrene solutions in EPC vesicles, which indicated that the excimers in pyrene crystals and the peptide–pyrene solution were static excimers resulting from pyrene molecules that were pre-associated in solid pyrene crystals. The excimers of pyrene and peptide–pyrene solutions in EPC vesicles were dynamic excimers which were formed via diffusion of dispersed pyrene molecules [33].

To further investigate the transfer of pyrene from the peptide coating into the EPC vesicles, we determined the steady-state fluorescence spectra of peptide–pyrene solutions with EPC vesicles shortly after sample preparation. Previously, Winnik et al. [34] used time-based fluorescence scans to monitor the increase in monomer emission as a function of time, a method that can be used in our system. Therefore, to observe the transfer of the pyrene in the EPC–peptide–pyrene solution more precisely, we
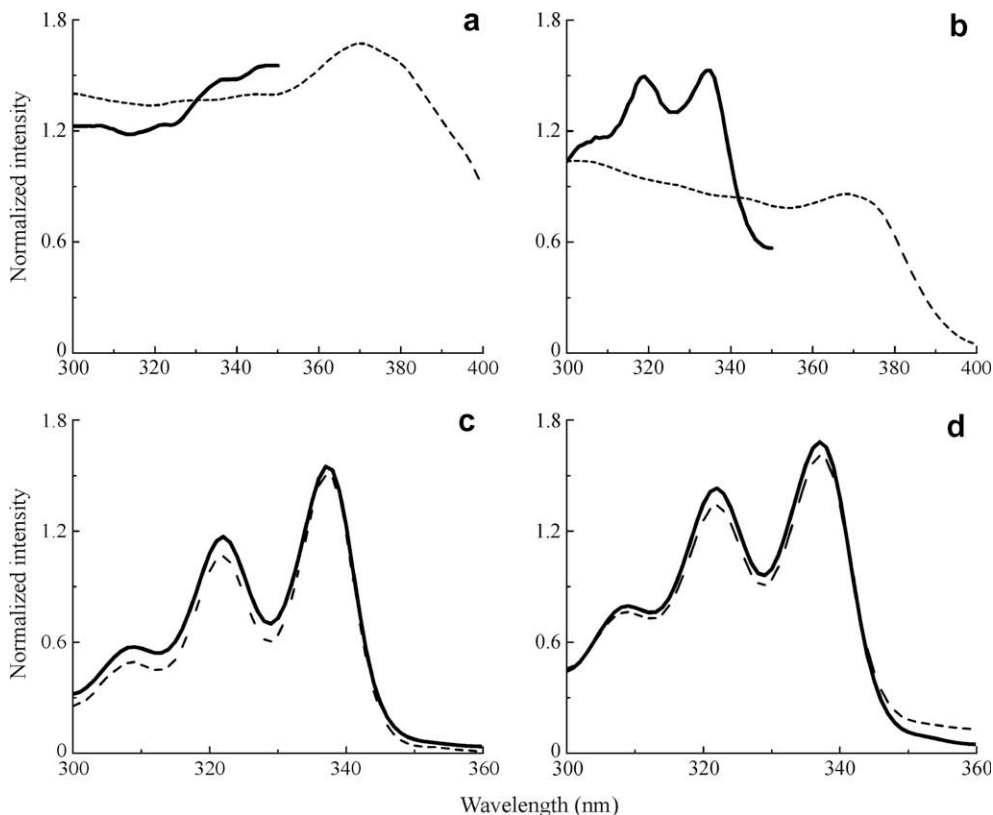
Fig. 4. Normalized fluorescence excitation spectra for solid pyrene crystals (a), peptide–pyrene solution ([Py] = 4.45 × 10^{-3} M, [Peptide] = 3.79 × 10^{-4} M) (b), pyrene in EPC vesicles ([Py] = 5.00 × 10^{-5} M) (c), and the peptide–pyrene solution mixed with EPC vesicles ([Py] = 4.45 × 10^{-5} M, [Peptide] = 3.79 × 10^{-6} M) (d). The emission wavelength (λ_{em}) was 374 nm (—) and 470 nm (– – –).

monitored the intensity (I_m) of the pyrene monomer as a function of time at an emission wavelength of 374 nm over a period of 4 h at 2-s intervals. As determined from the spectra, the I_1/I_3 ratio was 1.1, which indicated that the pyrene monomer was always located inside the hydrophobic vesicle membrane. Two profiles are shown in Fig. 5. Profiles 1 and 2 represent the release of pyrene from the peptide solution into the EPC vesicles at final pyrene concentrations of 1.48 × 10^{-5} and 7.40 × 10^{-5} M, respectively. Profile 1, at a low pyrene concentration, exhibits a continuous increase in I_m during the first half hour, reaching a plateau after 2 h. This indicates that, when the peptide–pyrene solution was added to the EPC vesicles, the concentration of pyrene monomers increased as the pyrene crystals were transferred into the EPC vesicles, and the likelihood for pyrene to absorb a photon increases in the transition from the crystalline form to the monomer. Correspondingly, I_m reached a plateau when all of the pyrene molecules were dissolved into the vesicles. Profile 2, as obtained at a higher concentration of pyrene, shows a sharp increase in I_m to a maximum after 24 min, which was followed by a continuous decrease to a plateau that was reached after about 1.5 h. Accordingly, if too much pyrene was added to the liposome solution, the dissolution of pyrene molecules in the EPC vesicles lead to greater pyrene absorption. After the pyrene concentration in the lipo-
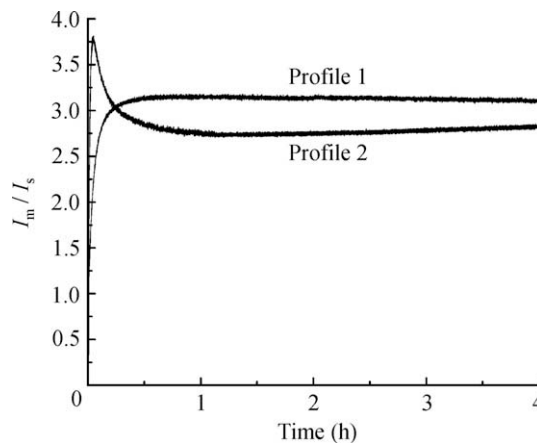

Fig. 5. Fluorescence emission intensity of the pyrene monomer as a function of time for release of pyrene from the peptide coating into EPC vesicles. The excitation wavelength was 336 nm, and the emission wavelength was 374 nm. The emission intensity (I_m) was divided by that of the standard (I_s). Profile (1): data obtained over 4 h at 2-s intervals ([Py] = 1.48 × 10^{-5} M, [Peptide] = 1.26 × 10^{-6} M, [EPC] = 6.99 × 10^{-4} M). Profile (2): data obtained over 4 h at 2-s intervals ([Py] = 7.40 × 10^{-5} M, [Peptide] = 6.30 × 10^{-6} M, [EPC] = 6.99 × 10^{-4} M).

somes reaches a critical level, the inner filter effect takes place [35], which leads to decreased fluorescence of the pyrene monomer until the crystals were fully dissolved and a

plateau was reached. It was reported that there are several other factors that could affect these profiles, such as self-quenching of the pyrene monomers and multiple scattering with the EPC vesicles. However, the pyrene crystals were often larger than the EPC vesicles, and self-quenching was more likely to occur through the diffusional encounter with another pyrene molecule dissolved in the liposome bilayer. Consequently, these factors are expected to be static with respect to the dissolution of the pyrene molecules in the lipid bilayer. Multiple scattering might also be present, but it would be expected to be greatly reduced because we used the same liposome system for the calibration curve and for the release experiments.

3.3. Generation of the calibration curve

A calibration curve was generated to obtain quantitative information of the amount of pyrene to be transferred into the liposome and was based on the data shown in Fig. 5. A series of solutions of pyrene in EPC vesicles were prepared with pyrene concentrations ranging from 1.0×10^{-6} to 1.3×10^{-5} M. The fluorescence intensity of the pyrene monomer divided by that of the standard to account for lamp fluctuations (I_m/I_s) is shown in Fig. 6 as a function of the pyrene concentration. The calibration curves also revealed the inner filter effect as I_m/I_s passes through a maximum, with little changes for pyrene concentrations between 2.0×10^{-5} and 3.0×10^{-5} M. Therefore, a gap was observed in the time-dependent concentration profile for pyrene located inside the vesicles, where no data points were reported for pyrene concentrations in this range. Two functions of I_m/I_s fitted for different pyrene concentration ranges were obtained, and showed good fit with a sigmoidal function. At concentrations of pyrene up to 2.5×10^{-5} M, the monomer intensity was fit with a sigmoidal function, where $I_m/I_s = 3.810 - 99.634/(1 + e^{([Py]+20.245/6.233)})$, ($R^2 = 0.9920$). Another sigmoidal function, $I_m/I_s = 0.558 + 5.280/(1 + e^{([Py]-40.081/29.308)})$, ($R^2 =$
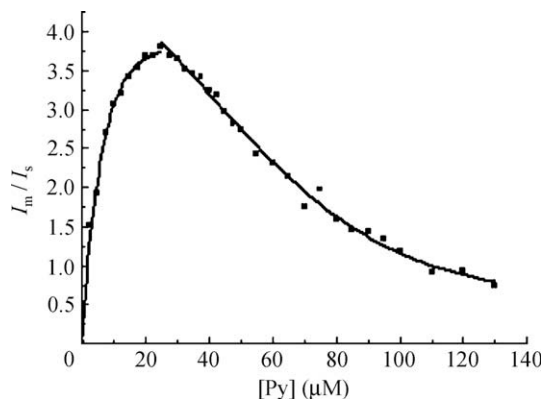
Fig. 6. Calibration curve for different pyrene concentrations in EPC vesicles ([EPC] = 6.99×10^{-4} M). The fluorescence intensity (I_m) was divided by that of the standard (I_s) to account for lamp fluctuations.
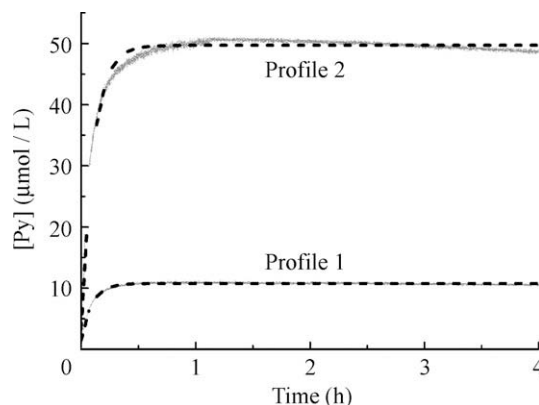
Fig. 7. Profiles for the release of molecular pyrene from peptide-coated pyrene crystals into a solution of EPC vesicles according to fluorescence results. The continuous dots represent the actual pyrene concentration, and the dashed line was the data fitted with a sigmoidal function.

0.9936) was used to fit the monomer intensity for higher pyrene concentrations.

By transforming the I_m/I_s-versus-time profiles with a calibration curve of I_m/I_s-versus-concentration of pyrene in EPCs, we developed a release curve of the concentration-versus-time profiles of pyrene from the peptide carrier into EPC vesicles, as shown in Fig. 7. Over time, more pyrene molecules were transferred from the peptide–pyrene solution into the EPC vesicles, reaching a plateau as the pyrene molecules were fully dissolved. The final pyrene concentrations of Profiles 1 and 2 were about 10.7 and 48.7 μM, respectively (Fig. 7). To describe the transfer of pyrene from peptide into EPC vesicles, a release constant is required. Although it is difficult to establish a model describing the uniqueness of the pyrene transfer, the profiles shown in Fig. 7 could be fit with Eq. (1), where $[PY](t)$, $[PY]_{eq}$, and $[PY]_0$ represent the pyrene concentration inside the EPC vesicles at time t, at equilibrium (infinite time), and at time $t = 0$ s, respectively. The k_{trans} of profile 1 and profile 2 of Fig. 7 were 3.32 ± 0.1/h and 3.51 ± 0.1/h, respectively.

$$[PY](t) = [PY]_{eq} - ([PY]_{eq} - [PY]_0) \exp(-k_{trans} \times t) \qquad (1)$$

4. Conclusions

In the present study, we demonstrate that the novel designed peptide, Ac-RADAGAGARADAGAGA-NH$_2$, can stabilize the crystals of a hydrophobic model compound by mechanical stirring and forms a colloidal suspension. The steady-state fluorescence spectra of the peptide–pyrene solution and the peptide–pyrene solution in the presence of EPCs showed that the pyrene crystals were molecularly dissolved in the vesicular membrane. The release behavior of pyrene into the EPC vesicles was investigated by steady-state fluorescence spectra, and the pyrene concentration in the EPC vesicles was determined as a function of time. We also determined the concentration of pyrene in EPC vesicles by comparing the monomer signal with that of a calibration curve. The transfer rate

constants were also determined to quantify the transfer behavior of pyrene into EPC vesicles. Our results suggest that pyrene can be transferred into the lipid bilayers from the novel designed amphiphilic peptide, and that the peptide is a potential carrier for low molecular weight, water-insoluble compounds.

Acknowledgements

References

[1] Zhang S, Holmes TC, Lockshin C, et al. Spontaneous assembly of a self-complementary oligopeptide to form a stable macroscopic membrane. Proc Natl Acad Sci USA 1993;90(8):3334–8.

[2] Zhang S. Emerging biological materials through molecular self-assembly. Biotechnol Adv 2002;20(5–6):321–39.

[3] Zhang S, Altman M. Peptide self-assembly in functional polymer science and engineering. React Funct Polym 1999;41(1–3):91–102.

[4] Zhang S, Marini DM, Hwang W, et al. Design of nanostructured biological materials through self-assembly of peptides and proteins. Curr Opin Chem Biol 2002;6(6):865–71.

[5] Zhang S, Holmes TC, DiPersio CM, et al. Self-complementary oligopeptide matrices support mammalian cell attachment. Biomaterials 1995;16(18):1385–93.

[6] Holmes TC, Lacalle S, Su X, et al. Extensive neurite outgrowth and active synapse formation on self-assembling peptide scaffolds. Proc Natl Acad Sci USA 2000;97(12):6728–33.

[7] Zhang S, Gelain F, Zhao X. Designer self-assembling peptide nanofiber scaffolds for 3D tissue cell cultures. Semin Cancer Biol 2005;15(5):413–20.

[8] Davis ME, Motion JP, Narmoneva DA, et al. Injectable self-assembling peptide nanofibers create intramyocardial microenvironments for endothelial cells. Circulation 2005;111:442–50.

[9] Zhang S, Yan L, Altman M, et al. Biological surface engineering: a simple system for cell pattern formation. Biomaterials 1999;20(13):1213–20.

[10] Zhao X, Nagai Y, Reeves PJ, et al. Designer short peptide surfactants stabilize G protein-coupled receptor bovine rhodopsin. Proc Natl Acad Sci USA 2006;103(47):17707–12.

[11] Nagai Y, Unsworth LD, Koutsopoulos S, et al. Slow release of molecules in self-assembling peptide nanofiber scaffold. J Control Release 2006;115(1):18–25.

[12] Keyes-Baig C, Duhamel J, Fung SY, et al. Self-assembling peptide as a potential carrier of hydrophobic compounds. J Am Chem Soc 2004;126(24):7522–32.

[13] Fung SY, Yang H, Chen P. Formation of colloidal suspension of hydrophobic compounds with an amphiphilic self-assembling peptide. Colloid Surface B 2007;55(2):200–11.

[14] Chen JY, Minoura N, Tanioka A. Transport of pharmaceuticals through silk fibroin membrane. Polymer 1994;35(13):2853–6.

[15] Hino T, Tanimoto M, Shimabayashi S. Change in secondary structure of silk fibroin during preparation of its microspheres by spray-drying and exposure to humid atmosphere. J Colloid Interface Sci 2003;266(1):68–73.

[16] Tsukada M, Freddi G, Minoura N, et al. Preparation and application of porous silk fibroin materials. J Appl Polym Sci 1994;54(4):507–14.

[17] Iizuka E. Degree of crystallinity and modulus relationships of silk thread from cocoons of *Bombyx mori* L. and other moths. Biorheology 1965;3(1):1–8.

[18] Hayashi CY, Shipley NH, Lewis RV. Hypotheses that correlate the sequence, structure, and mechanical properties of spider silk proteins. Int J Biol Macromol 1999;24:271–5.

[19] Kaplan D, Adams WW, Farmen B, et al. Silk polymers. Washington, DC: American Chemical Society; 1994, p. 370.

[20] Zhang S, Lockshin C, Cook R, et al. Unusually stable β-sheet formation in an ionic self-complementary oligopeptide. Biopolymers 1994;34(5):663–72.

[21] Horii A, Wang X, Gelain F, et al. Biological designer self-assembling peptide nanofiber scaffolds significantly enhance osteoblast proliferation, differentiation and 3-D migration. PLoS ONE 2007;2:e190.

[22] Ellis-Behnke RG, Liang YX, You SW, et al. Nano neuro knitting: peptide nanofiber scaffold for brain repair and axon regeneration with functional return of vision. Proc Natl Acad Sci USA 2006;103(13):5054–9.

[23] Wilhelm M, Zhao CL, Wang Y, et al. Poly (styrene-ethylene oxide) block copolymer micelle formation in water: a fluorescence probe study. Macromolecules 1991;24(5):1033–40.

[24] Kelly SM, Jess TJ, Price NC. How to study proteins by circular dichroism. Biochim Biophys Acta 2005;1751(2):119–39.

[25] Wang G, Geng ML. Unfolding of apomyoglobin studied with two-dimensional correlations of tryptophan, 8-anilino-1-naphthalenesulfonate, and pyrene fluorescence. J Mol Struct 2006;799(1–3):177–87.

[26] Winnik FM. Photophysics of preassociated pyrenes in aqueous polymer solutions and in other organized media. Chem Rev 1993;93(2):587–614.

[27] Mizusaki M, Morishima Y, Winnik FM. An assessment by fluorescence spectroscopy of the stability of polyanions/positively charged liposome systems in the presence of polycations. Polymer 2000;142:5615–24.

[28] Kalyanasundaram K, Thomas JK. Environmental effects on vibronic band intensities in pyrene monomer fluorescence and their application in studies of micellar systems. J Am Chem Soc 1997;99(7):2039–44.

[29] Zachariasse KA, Duveneck G, Busse R. Intramolecular excimer formation with 1,3-di(1-pyrenyl) propane. Decay parameters and influence of viscosity. J Am Chem Soc 1984;106(4):1045–51.

[30] Ringsdorf H, Venzmer J, Winnik FM. Interaction of hydrophobically-modified poly-*N*-isopropylacrylamides with model membranes or playing a molecular accordion. Angew Chem Int Ed Engl 1991;30(3):315–8.

[31] Pandey S, Redden RA, Hendricks AE, et al. Characterization of the solvation environment provided by dilute aqueous solutions of novel siloxane polysoaps using the fluorescence probe pyrene. J Colloid Interface Sci 2003;262(2):579–87.

[32] Gao C, Qian H, Wang S, et al. Self-association of hyperbranched poly (sulfone-amine) in water: studies with pyrene-fluorescence probe and fluorescence label. Polymer 2003;44(5):1547–52.

[33] Vigil MR, Bravo J, Atvars TD, et al. Photochemical sensing of semicrystalline morphology in polymers: pyrene in polyethylene. Macromolecules 1997;30(17):4871–6.

[34] Winnik FM, Adronov A, Kitano H. Pyrene-labeled amphiphilic poly-(*N*-isopropylacrylamides) prepared by using a lipophilic radical initiator: synthesis, solution properties in water, and interactions with liposomes. Can J Chem 1995;73:2030–40.

[35] Lakowicz JR. Principles of fluorescence spectroscopy. New York: Plenum Press; 1983, p. 44–5.